Eur. Phys. J. B **46**, 201–205 (2005)
DOI: 10.1140/epjb/e2005-00246-8

THE EUROPEAN PHYSICAL JOURNAL B

Electron spin resonance of Eu^{2+} in the Eu doped clathrate Ba_6Ge_{25}

J. Sichelschmidt[1,a], W. Carrillo-Cabrera[1], V.A. Ivanshin[1,2], Yu. Grin[1], and F. Steglich[1]

[1] Max Planck Institute for the Chemical Physics of Solids, 01187 Dresden, Germany
[2] MRS Laboratory, Kazan State University, 420008 Kazan, Russia

Received 19 November 2004 / Received in final form 18 March 2005
Published online 11 August 2005 –

Abstract. We report electron spin resonance (ESR) investigations of the clathrate compound $Ba_{6-x}Eu_xGe_{25}$ ($x = 0.03$–0.4) which exhibits a temperature induced, two-step reconstructive structure transformation at temperatures between 185 K and 223 K. The linewidth of the Eu^{2+} ESR proves to be sensitive to the transformation. Another anomaly in the temperature dependence of the linewidth is found near $T = 60$ K which points towards another possible structural transition. Both anomalies seen in the ESR linewidth are not sensitive to the Eu content in contrast to the strong Eu-concentration dependence of transport properties.

PACS. 76.30.-v Electron paramagnetic resonance and relaxation – 76.30.Kg Rare-earth ions and impurities

1 Introduction

Clathrate compounds belong to the class of so-called 'filled cage' systems where 'guest' atoms are loosely bound in oversized cages of a 3D framework formed by covalently bonded silicon, germanium or tin. These solid systems are believed to be basically new materials for effective thermoelectric devices as their properties combine glass-like heat conduction ('phonon glasses') with good electrical conduction ('electron crystals') [1]. Apart from their promising thermoelectric properties, clathrates may give the opportunity to study the physics of the new strongly correlated, low-density charge carrier systems [2,3] and therefore may provide a new class of small-gap semiconductors/semimetals ('Kondo Insulators', KI) [4]. In the clathrate I type structure, the guest site atoms could be fully occupied by Eu, however, a KI is still not obtained [5]. A partial guest site substitution with Eu was successfully done in the recently discovered clathrate IX type compound Ba_6Ge_{25} [6].

The cubic structure of Ba_6Ge_{25} is characterized by a 3D chiral framework of condensed Ge_{20} pentagonal dodecahedra (*pdod* cages) embedded in a 3D-channel zeolitelike labyrinth. Each Ge_{20} *pdod* cage is centered by a Ba atom (Ba1) while the cavities in the labyrinth are occupied by other Ba atoms, Ba2 in a distorted Ge_{20} polyhedral cavity and Ba3 in a cube-like Ge_8 cavity [6]. At temperatures $T_{S1} \simeq 223$ K and $T_{S2} \simeq 185$ K transport, magnetic and thermodynamic properties change drastically and show that Ba_6Ge_{25} undergoes a metal to semiconductor-like, broad two-step first-order phase transition [7]. Accurate single-crystal X-ray diffraction studies in the temperature range 95–295 K revealed a structural phase transition of reconstructive nature, which involves breaking of ≈28% of the Ge4–Ge6 bonds and Ba2 atom displacements [8] (for atoms labeling see Ref. [6,8]). This bond breaking results in the formation of new electron acceptors (three-bonded germanium species with dangling bonds) and the effective charge carrier concentration is then reduced, which affects the physical properties.

Below the phase transition the disorder, resulting from the random Ge–Ge bound breaking and Ba atom displacements, implies strong random scattering as important mechanism in the resistivity. The conduction carriers are assumed to propagate within the framework of *pdod* cages. Their density is relatively low as seen, for instance, in the optical properties which are characterized by a low plasma energy [9]. Ba_6Ge_{25} shows BCS-like superconductivity below $T_c \simeq 0.24$ K [7,10]. Investigations of the pressure dependence of T_c and the upper critical field have shown that the structural phase transition causes a significant reduction of the density of states at the Fermi energy N_{E_F} by a factor of about 4 [10,11]. The magnetic susceptibility of Ba_6Ge_{25} also shows a pronounced two-step decrease at T_{S1} and T_{S2} when lowering T. In total, it is diamagnetic which is associated with a dominating contribution from molecular ring currents induced by the Lorentz force in a magnetic field.

The mentioned pronounced effects of the phase transition on the electronic and magnetic properties could be explained by changes of the band structure at the phase transition. Band structure calculations revealed that below the phase transition the density of states (DOS) at

[a] e-mail: sichelschmidt@cpfs.mpg.de

the Fermi energy is strongly suppressed due to Ba2 and Ge4 atoms being shifted to split sites [12,13]. This effect occurs in the context of hybridization of Ba 5d states with Ge states and a significant contribution from Ba 5d states to N_{E_F}.

The hybridization may be investigated by the relaxation of magnetic ions doped into the framework and probed with the electron spin resonance (ESR) technique. Up to now, to our knowledge, ESR investigations of intermetallic clathrates have been performed only on sodium-containing clathrates, Na_xSi_{136} with $1.5 \leq x \leq 22$ [14, 15]. By ESR, Na single atoms as well as dimer cations Na_2^+ incorporated in the Si cages could be detected. The Na paramagnetic centers are isolated from the Si framework which results in an ESR linewidth of less than 1 mT. The thermal activation of Na electrons to the conduction band was revealed by a non-Curie type of the ESR intensity temperature dependence. Hence this ESR enabled a good estimation of the Na-donor level distance to the conduction band [15].

We investigated the ESR of Eu-doped Ba_6Ge_{25} where Eu atoms occupy partially two (Ba1, Ba3) of the three possible Ba positions in the crystal structure. Interpreting the ESR signal as the resonance of Eu^{2+} ions we focus on the temperature dependence of its linewidth ΔB. Two kinks in the temperature dependence of ΔB have been found: one near the structural phase transition at $T \simeq 175$ K and another at $T \simeq 60$ K. Both kinks signalize a change of magnetic relaxation which indicates a change of interaction between Eu 4f states and conduction electrons.

2 Experimental details and results

ESR probes the absorbed power P of a transversal magnetic microwave field as a function of an external static magnetic field B. To improve the signal-to-noise ratio, a lock-in technique is used by modulating the static field, which yields the derivative of the resonance signal dP/dB. The ESR experiments were performed at X-band frequencies ($\nu \approx 9.4$ GHz) with a BRUKER ELEXSYS 500 spectrometer. The temperature was varied between 2.7 K$\leq T \leq$ 295 K by using a He-flow cryostat.

The preparation and structural characterization of the polycrystalline $Ba_{6-x}Eu_xGe_{25}$ with $x = 0.03, 0.05, 0.1, 0.2, 0.4$ is described elsewhere [7,16]. For the ESR investigations the polycrystalline samples were powdered (grain size $\leq$ 20 μm). Full penetration of the microwave field through the sample grains at all temperatures is expected from the electrical resistivity values [7] and is verified by absence of dispersion contribution to the ESR Lorentzian lineshapes. An overview of ESR spectra of $Ba_{6-x}Eu_xGe_{25}$ is shown in Figure 1. Comparable spectra could not be detected in pure Ba_6Ge_{25}. Magnetization and magnetic susceptibility measurements [7] demonstrate that the Eu ion in $Ba_{6-x}Eu_xGe_{25}$ is in the $4f^7$ configuration (Eu^{2+}). Thus the observed ESR signals in $Ba_{6-x}Eu_xGe_{25}$ are undoubtedly related to the paramagnetic Eu^{2+} ion.

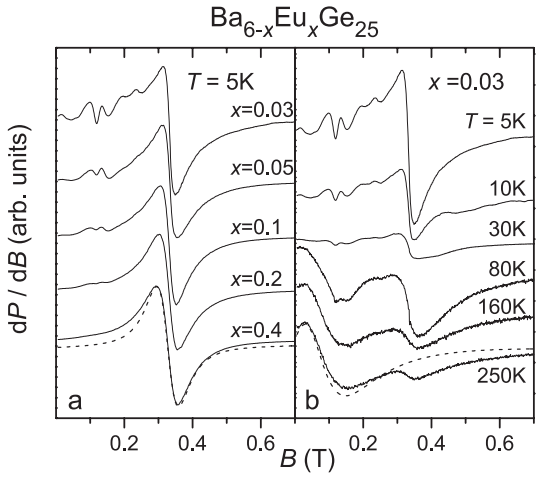

Fig. 1. Dependence of the ESR spectra of $Ba_{6-x}Eu_xGe_{25}$ on (a) the Eu concentration and (b) the temperature (here the spectra for $T \geq 80$ K are magnified by a factor of 10). The dashed line in frame (a) shows a single Lorentzian lineshape. In frame (b) the dashed line demonstrates the contribution of the background signal exemplarily at $T = 250$ K.

For the lowest Eu concentration ($x = 0.03$) we obtain the best resolution of fine structure in the ESR spectra, as shown in Figure 1a for $T = 5$ K. With increasing x the fine structure gets less pronounced until, at $x = 0.4$, the center line dominates the spectra. This effect may be explained by an increasing magnetic dipolar interaction between Eu^{2+} ions as their average distance is reduced by increasing their concentration. The center line has a peak-to-peak linewidth which increases by increasing Eu^{2+} concentration and which, at the highest concentration, can neither be described by a single Lorentzian line (dashed line in Fig. 1a), nor by a Gaussian line shape. Therefore, as a Lorentzian line shape is not observed, the effect of a narrowing process on the total ESR linewidth due to strong exchange coupling between the magnetic Eu^{2+} ions seems not to be realized. This so-called exchange narrowing causes resolved fine structure lines to draw together narrowing into a single line [17].

As shown in Figure 1b, by increasing temperature the fine structure resolution decreases which is a consequence of a thermal linewidth broadening of each fine structure line. The so-called Korringa relaxation of magnetic ions in metallic hosts [17] may be the origin for this broadening mechanism. The center line dominates the spectrum with decreasing intensity, until the background signal prevails for temperatures above ≈100 K, as the background signal at $T = 250$ K demonstrates in Figure 1b (dashed line).

When placing an Eu^{2+} ion ($^8S_{7/2}$ ground state) in a crystalline electric (ligand) field it exhibits at zero magnetic field a splitting of its electronic states which arises indirectly through relatively high order perturbation processes and which, doing an ESR experiment results in a fine structure in the resonance spectrum [18]. The ESR of Eu^{2+} with a $J = \frac{7}{2}$ manifold is then composed of seven allowed transitions $M \leftrightarrow M-1$ (M: electronic magnetic quantum number, $M = \frac{7}{2}, \frac{5}{2}, \frac{3}{2}, \frac{1}{2}, -\frac{1}{2}, -\frac{3}{2}, -\frac{5}{2}, -\frac{7}{2}$).

However, the observability of each of these transitions depends on the symmetry of the particular crystalline electric field and the orientation of the magnetic field respective the crystal axes. As we use polycrystalline samples of $Ba_{6-x}Eu_xGe_{25}$ one expects from the latter requirement a superposition of all the orientation dependent resonance fields of the seven transitions. Moreover, two Eu^{2+} species located in different crystalline electric fields exist in $Ba_{6-x}Eu_xGe_{25}$. For $x = 0.6$, the Eu atoms occupy partially the Ba1 sites and Ba3 sites at a ratio 1:2.2 [16]. Despite these effects of superposition the signatures of fine structure are well observed as demonstrated in Figure 2 which shows a spectrum with best obtained resolution, i.e. at the lowest possible temperature and the lowest Eu^{2+} concentration, $x = 0.03$. The dashed line, obtained by a numerical fitting procedure, describes the measured spectrum (dots) with 10 Lorentzian lines, leaving still small differences between the fit and experiment behind (hardly visible in Fig. 2). Clearly, due to above mentioned reasons, definite information on crystal-field parameters could only be obtained from ESR measurements on single-crystalline material.

Describing the $x = 0.03$ spectra with multiple (more than two) Lorentzian lines stops to produce reasonable results for $T > 10$ K. This is because the intensity of each single line reduces according to a Curie law and the center line with highest intensity remains and dominates the spectra. Therefore, in order to extract the temperature dependence of the spectra, we fitted them with two lines: one narrow (linewidth $\Delta B \sim 0.02$ T) central line and another broad ($\Delta B \sim 0.1$ T) line describing the remaining unresolved fine structure (see the solid line in Fig. 2). The ESR intensity I_{ESR} of the central line is determined by the area under the absorption $P(B)$. I_{ESR} is proportional to the static susceptibility of the Eu^{2+} spins. As demonstrated in the inset of Figure 2, $I_{\mathrm{ESR}}(T)$ follows a Curie law and shows no signs of magnetic ordering of the Eu^{2+} spins.

The ESR g value of $Ba_{6-x}Eu_xGe_{25}$ ($x = 0.03$) of the center line is $g = 2.02(0)$ (using the center line resonance field at $T = 2.7$ K). The g value expected for a Eu^{2+} in a isolating environment of cubic crystalline field symmetry is $g^{iso} = 1.9935$ [18]. For the isothermal ESR of local moments on metallic hosts a deviation of the experimental g value from g^{iso} is expected and is due to the local moment – conduction electron exchange interaction [19].

As the spectrum is a superposition of several (more than 10) overlapping resonances it was not possible to obtain a clear and accurate temperature dependence of the center resonance field and hence of the g value. The center line varies its position less than 2% when changing the temperature between 300 K and 4.2 K. Especially, at the phase transition temperatures no pronounced anomaly of the main g value is visible. The latter could have been expected because the total magnetic susceptibility shows a huge jump at T_{S1} and T_{S2} [7]. Also the strongly magnetic field dependent low-T upturn of the magnetic susceptibility does not show up in the g value. The lack of these anomalies suggests that the static magnetic field

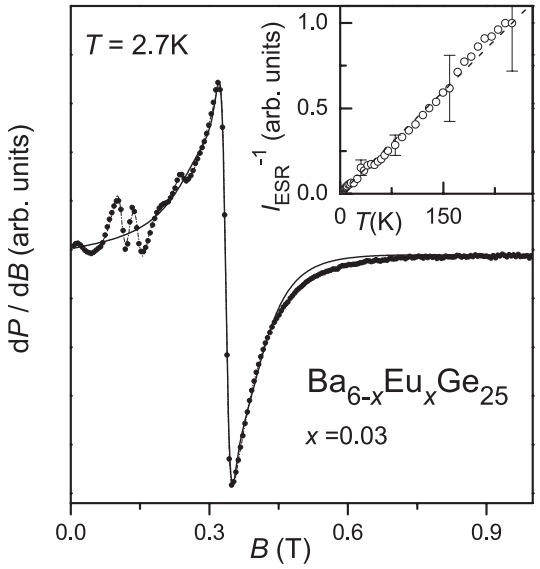

Fig. 2. ESR spectrum (solid circles) of $Ba_{6-x}Eu_xGe_{25}$ ($x = 0.03$) at the lowest temperature. The dashed line fits the data with 10 Lorentzian lines. The solid line models the spectrum with two Lorentzian lines: a narrow central line and a broader line describing the remaining unresolved fine structure. Inset: Temperature dependence of reciprocal ESR intensity I_{ESR} of the central fit-line. The dashed line is a linear fit corresponding to a Curie law.

distribution at the guest atom, which is picked up by the ESR g value of the ion Eu^{2+} at the guest site, is only weakly influenced by the magnetic field changes within the *pdod* cage network.

The ESR linewidth ΔB (here measured as the half width at half maximum of $P(B)$) proved to be the only quantity which yields obvious anomalies in its temperature dependence. Figure 3 shows for all investigated Eu^{2+} concentrations the resulting ΔB. The data were obtained by fitting the spectra with two Lorentzian lines as described above and as shown for $x = 0.03$ in Figure 2.

Three regions of different temperature dependencies of the linewidth may be determined. The dashed lines in Figure 3 mark these regions. The first region at $T < 60$ K shows a T-linear behavior of ΔB with a slope of 0.4 mT/K for all x. In the second region, 60 K $< T <$ 175 K, the linear slope is clearly reduced, less pronounced for $x = 0.05$, and most clearly for $x = 0.03$. Increasing T towards the third region, above ≈175 K, the slope further reduces but much more smooth than the transition at 60 K. The third region is characterized for $x = 0.2$ and $x = 0.4$ by a negative slope, −0.2 mT/K, of the T-linear behavior of $\Delta B(T)$. For $x < 0.2$ the linewidth is T-independent for $T > 175$ K. Hysteresis effects which are clearly found in susceptibility and resistivity near $T_{S2} = 185$ K ($x = 0$) [7] could not be observed in the temperature dependence of the ESR linewidth probably because of the large linewidth and multiple line superposition which inhibits a sufficient resolution. Near the temperature $T_{S1} = 223$ K no anomalous behavior of the linewidth could be observed.

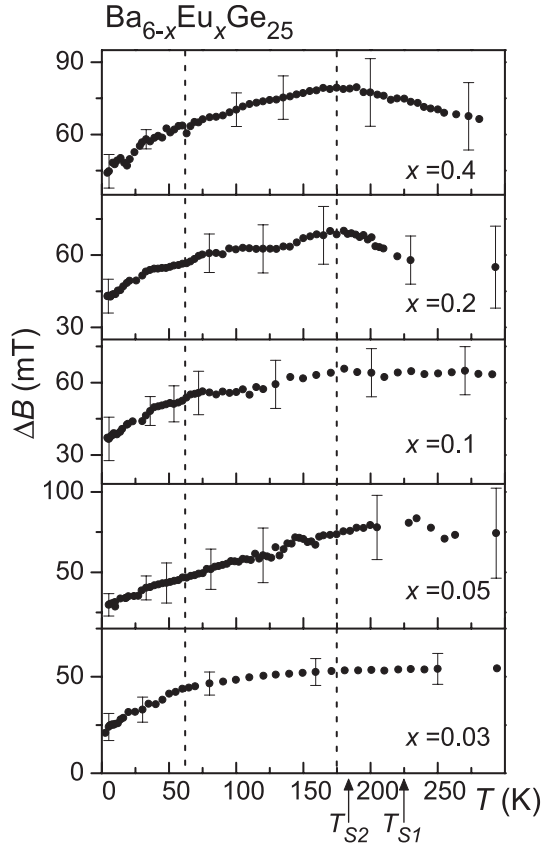

Fig. 3. Temperature dependencies of the ESR linewidth ΔB, obtained by fitting the center line of the spectra with a single Lorentzian line. The vertical dashed lines mark the T-regions where the average slope of $\Delta B(T)$ changes. The arrows at T_{S1} and T_{S2} mark the temperatures between which a two-step reconstructive structure transformation occurs.

3 Discussion

Performing ESR on Eu^{2+} doped on the Ba(1) and Ba(3) sites in Ba_6Ge_{25} allows direct characterization of the magnetic properties at these sites. The temperature dependencies below $T \simeq 175$ K of the linewidth is consistent with a local moment ESR in a metallic environment where a relaxation via the conduction-localized electron exchange mechanism dominates [19], hereafter called "metallic relaxation" which causes with increasing T a linear-in-T increase of $\Delta B(T)$. This perspective is further justified by the clear metallic character of the charge dynamics as seen in the far-infrared optical properties of Ba_6Ge_{25} [9].

Although the ESR below $T \simeq 175$ K shows characteristics typical for metals the resistivity displays "bad metal" behavior ($\rho_0 \simeq 1.5$ mΩcm), i.e. localization effects become important [10], resulting in a small temperature gradient. On the other hand, in a T regime where the resistivity shows metallic behavior with a positive temperature gradient ($T > T_{S1}$), the ESR linewidth shows the tendency to decrease with increasing T.

Crossing the temperatures T_{S1} and T_{S2} one observes a reconstructive structure transformation. This leads to changes in the electronic band structure and N_{E_F} [12] which is also nicely seen in the optical conductivity [13]. The ESR line broadening due to metallic relaxation includes a slope of the T-linear $\Delta B(T)$ which is proportional to $(J \cdot N_{E_F})^2$ [17]. Here J denotes the exchange coupling constant of the local moments with the conduction electron spins. Hence, metallic relaxation is sensitive to changes in N_{E_F} and, because of J, to changes of the distance between the local moment and conduction electrons. Therefore the above mentioned structural effects with concomitant changes in band structure can explain the slope changes in the temperature dependence of the Eu^{2+} ESR linewidth if metallic relaxation is involved.

The absence of any visible linewidth anomaly near T_{S1} and the clear change of slope near T_{S2} further supports the relevance of structural effects on the ESR linewidth. According to the details of the structural transition [8] the transition near T_{S1} mostly involves Ba2 atoms. The Ba1 and Ba3 atoms are noticeably displaced not until T_{S2} is reached. Thus, because the Eu^{2+} ions occupy only Ba1 and Ba3 sites, a distinct effect on the ESR linewidth would not be expected until the temperature is reduced below T_{S2}.

The linewidth kink near $T = 60$ K has a counterpart seen as anomalies in susceptibility, resistivity and thermal conductivity [7]. We propose that this temperature marks another change in the density of states at the Fermi energy which may be caused by changes in electronic band structure. Indeed, near $T = 60$ K, the band structure changes have recently been observed by optical conductivity investigations. Recent low temperature structural investigations indicate another structural reconstruction in the Ge *pdod* [20], further supporting these band structure effects.

Comparing the ESR results with the transport properties of $Ba_{6-x}Eu_xGe_{25}$ reveals a partly disparate behavior. Enhancing the Eu concentration leads to a suppression of the phase transition $S1$ and $S2$ seen in the resistivity while no corresponding suppression of the boundary at $T \simeq 175$ K is visible in the ESR-parameters (Fig. 3). The reasons for this discrepancy might again be related to the sensitivity of the metallic relaxation to local moment conduction electron distances. Below $T_{S1,S2}$ the Eu^{2+} on the Ba1 site located in the Ge_{20} *pdod* cage, $(Eu1)^{2+}$, are closer to the Ge framework than the Eu^{2+} on the Ba3 site located at an open framework position, $(Eu3)^{2+}$. Moreover, the $(Eu3)^{2+}$ spins are mostly surrounded by Ge atoms which keep excess charges in dangling bonds [8] instead of contributing electrons to the conduction band. Therefore, between local spins and mobile charge carriers, a stronger exchange coupling for the $(Eu1)^{2+}$ spins than for the $(Eu3)^{2+}$ spins can be expected. Thus, it appears that the changes of slopes near 60 K and 175 K might most strongly be influenced by relaxation changes for the $(Eu1)^{2+}$ spin. The phase transition at T_{S1} and T_{S2} is mainly related to an increase of displacements at the Ba2 and Ba3 sites. Hence, the shifting of the phase transition due to Eu-doping towards lower temperatures is less affecting the Ba1 sites, being, however, the sites for Eu^{2+} with the most effective ESR metallic relaxation.

4 Summary and conclusion

We present ESR results of Eu^{2+} doped on the Ba1 and Ba3 sites in Ba_6Ge_{25}. The spectra contain a complex superposition of multiple lines due to fine structure splitting of Eu^{2+} which moreover are caused by different local atomic configurations being oriented arbitrarily in the magnetic field due to the use of polycrystalline samples. Therefore, for analysis, we restricted our discussion of the ESR parameters to the central, most intense line and mainly analyzed the temperature dependence of the ESR linewidth $\Delta B(T)$.

In agreement with previous magnetic susceptibility data [7], we found no signatures of magnetic ordering of Eu^{2+} spins down to the lowest accessible temperatures of 2.7 K. $\Delta B(T)$ shows changes of slopes at $T \simeq 60$ K and $T \simeq 175$ K. The temperature dependence of the structural details, especially those of the Ge_{20} pentagon dodecahedral cage and Ba displacements [8], proves to be consistent with the ESR results. The shifting of the structural phase transitions by Eu-doping towards lower temperatures, as seen in the electrical resistivity, does not produce corresponding changes of any ESR parameters. Treating the observed spectra as ESR of local moments in a metallic host, the slope changes in $\Delta B(T)$ are due to changes of the local moment conduction electron exchange as well as to changes of the density of states at the Fermi energy. The latter has been shown to be the result of changes in electronic band structure [13], which is detected by ESR most effectively by the Eu^{2+} ion at the Ba1 site.

References

1. G.A. Slack, in *CRC Handbook of Thermoelectrics*, edited by D.M. Rowe (Chemical Rubber, Boca Raton, FL, 1995), Chap. 34
2. S. Paschen, M. Baenitz, V.H. Tran, A. Rabis, F. Steglich, W. Carrillo-Cabrera, Yu. Grin, A.M. Strydom, P. de V. du Plessis, J. Phys. Chem. Solids **63**, 1183 (2002)
3. F. Steglich, A. Bentien, M. Baenitz, W. Carrillo-Cabrera, F.M. Grosche, C. Langhammer, S. Paschen, G. Sparn, V.H. Tran, H.Q. Yuan, Yu. Grin, Physica B **318**, 97 (2002)
4. G. Aeppli, Z. Fisk, Comments Cond. Mat. Phys. **16**, 155 (1992)
5. S. Paschen, W. Carrillo-Cabrera, A. Bentien, V.H. Tran, M. Baenitz, Yu. Grin, F. Steglich, Phys. Rev. B **64**, 214404 (2001)
6. W. Carrillo-Cabrera, J. Curda, H.G. von Schnering, S. Paschen, Yu. Grin, Z. Kristallogr. NCS **215**, 207 (2000)
7. S. Paschen, V.H. Tran, M. Baenitz, W. Carrillo-Cabrera, Yu. Grin, F. Steglich, Phys. Rev. B **65**, 134435 (2002)
8. W. Carrillo-Cabrera, H. Borrmann, S. Paschen, M. Baenitz, F. Steglich, Yu. Grin, J. Solid State Chem. **178**, 715 (2005)
9. J. Sichelschmidt, V. Voevodin, S. Paschen, W. Carrillo-Cabrera, Yu. Grin, F. Steglich, Acta Phys. Polonica B **34**, 613 (2003)
10. F.M. Grosche, H.Q. Yuan, W. Carrillo-Cabrera, S. Paschen, C. Langhammer, F. Kromer, G. Sparn, M. Baenitz, Yu. Grin, F. Steglich, Phys. Rev. Lett. **87**, 247003 (2001)
11. H.Q. Yuan, F.M. Grosche, W. Carrillo-Cabrera, V. Pacheco, G. Sparn, M. Baenitz, U. Schwarz, Yu. Grin, F. Steglich, Phys. Rev. B **70**, 1 (2004)
12. I. Zerec, A. Yaresko, P. Thalmeier, Yu. Grin, Phys. Rev. B **66**, 045115 (2002)
13. I. Zerec, W. Carrillo-Cabrera, V. Voevodin, J. Sichelschmidt, F. Steglich, Yu. Grin, A. Yaresko, S. Kimura, Phys. Rev. B **72**, 045122 (2005)
14. S.B. Roy, K.E. Sim, A.D. Caplin, Phil. Mag. B **65**, 1445 (1992)
15. H. Yahiro, K. Yamaji, M. Shiotani, S. Yamanaka, M Ishikawa, Chem. Phys. Lett. **246**, 167 (1995)
16. W. Carrillo-Cabrera, R. Cardoso Gil, S. Paschen, Yu. Grin, Z. Kristallogr. NCS **218**, 397 (2003)
17. S.E. Barnes, Adv. Phys. **20**, 801 (1981)
18. A. Abragam, B. Bleaney, *Electron Paramagnetic Resonance of Transition Ions* (Clarendon Press, Oxford, 1970)
19. R.H. Taylor, Adv. Phys. **24**, 681 (1975)
20. Analysis of the X-ray powder diffraction data at $T = 8$ K suggests that the dangling-bond character of the three-bonded Ge4 (created at $180 < T < 230$ K) is changed from a sp^3 towards a planar sp^2 configuration